Article

Not peer-reviewed version

Long-Range Imaging of Alpha Emitters Using Radioluminescence in Open Environments: Daytime and Nighttime Applications

Lingteng Kong *, Thomas Bligh Scott , John Charles Clifford Day , David Andrew Megson-Smith

Posted Date: 17 July 2024

doi: 10.20944/preprints202407.1264.v1

Keywords: Alpha Radiation Detection; Radio-luminescnece; Alpha Fluorescence; Long-Distance Monitoring; Solar Blind detector.

Article

Long-Range Imaging of Alpha Emitters Using Radioluminescence in Open Environments: Daytime and Nighttime Applications

Lingteng Kong *, Thomas Bligh Scott, John Charles Clifford Day and David Andrew Megson-Smith

HH Wills Physics Laboratory, Interface Analysis Centre, School of Physics, University of Bristol, Tyndall Avenue, Bristol BS8 1TL, UK; t.b.scott@bristol.ac.uk (T.B.S.); john.day@bristol.ac.uk (J.C.C.D.); david.megson-smith@bristol.ac.uk (D.A.M.-S.)
* Correspondence: jn19830@bristol.ac.uk; Tel.: +44-1174556650

Abstract: Alpha emitters like plutonium pose severe health risks when ingested, damaging DNA and potentially causing cancer. Traditional detection methods require proximity within millimeters of the contamination source, presenting safety risks and operational inefficiencies. Long-range detection through alpha radioluminescence (RL) offers a promising alternative. However, most of the previous experiments have been carried out under controlled conditions that preclude the overwhelming effect of ambient light. This study demonstrates successful detection of a 3 MBq alpha emitter in an open environment using a newly developed, lightweight compact alpha camera. This camera incorporates a deep-cooled CCD and a specially designed lens system with a low f-number to maximum the signal intensity. The lens was also designed to minimize blue shift effects of filters. Nighttime imaging was achieved with a dual-filter system using a sandwich filters assembly centered at 337 nm and 343 nm for capturing alpha RL and subtracting background light, respectively. At night, the alpha source was detected from 1 meter away within one minute. The system was also evaluated under simulated urban lighting conditions. For daytime imaging, a stack of tilted 276 nm short pass filters minimized sunlight interference, enabling clear detection of the alpha source at 70 cm within 10 minutes under indirect sunlight. This research not only underscores the viability of long-range optical detection of alpha emitters for environmental monitoring and scientific research but also highlights its ability to enhance nuclear safety and public health in real-world settings.

Keywords: alpha radiation detection; radio-luminescnece; alpha fluorescence; long-distance monitoring; solar blind detector

1. Introduction

Alpha particles, consisting of two protons and two neutrons, are identical to the nucleus of a helium-4 atom. They are typically emitted through the alpha decay of heavy nuclei, where an unstable atom releases an alpha particle to transform into a different element. The travel range of alpha particles in air is generally limited to several centimeters, depending on their energy, which makes detection challenging [1]. The ingestion of alpha emitters can cause severe DNA damage due to the high linear energy transfer (LET) characteristic of alpha particles. Alpha radiation deposits significant energy over a short track length, causing dense ionization along its path and substantial biological damage [2]. Additionally, alpha radiation can have a broader biological impact through the 'bystander effect,' where non-irradiated cells near irradiated ones also exhibit damage [3]. This was tragically highlighted by the poisoning of Alexander Litvinenko with polonium-210 [4]. Consequently, effective detection of alpha particles is crucial for protecting public health and the environment from the dangers of alpha radiation.

Current commercial hand-held alpha radiation monitors, such as Geiger-Mueller counters and scintillator detectors, require direct proximity to the radioactive source for accurate measurement, typically within millimeters of the contamination area. This process usually requires meticulous and repeated scanning of an area to ensure no contamination is missed, making the detection process labor-intensive and time-consuming. Such procedures not only increase the risk of contamination and dose uptake for workers but also escalate the costs associated with decontaminating or replacing

 doi:10.20944/preprints202407.1264.v1

contaminated equipment. For instance, following the assassination of Alexander Litvinenko, manual use of handheld alpha scanners was necessary to evaluate the spread of radioactive materials across more than 40 sites in London, demanding substantial human resources and time.

Recent advancements in the long-range detection of alpha emitters through radioluminescence (RL) have shown great promise for overcoming the limitations of close range alpha radiation monitoring [5,6,6–18]. This technique leverages the ionization of air molecules by alpha particles. The ionization process releases secondary electrons that excite surrounding nitrogen molecules, emitting photons as they return to their ground state. These photons, primarily in the 280–440 nm range, can travel hundreds of kilometers, detectable by optical instruments like photomultiplier tubes (PMT) and charge-coupled devices (CCD) [17,19,20]. The main emission peak at 337.1 nm, accounts for 25.7% of total emission [20].

However, the primary challenge in detecting alpha RL is the weak emission intensity. A single 5 MeV alpha particle typically generates only about 100 photons in air, which is over 10^{10} times lower than that of ambient light sources [11,21]. Therefore, most of the previous attempts for detecting alpha RL were carried under dark or specific light conditions without UV background.

For an imaging detector such as a CCD, which is usually sensitive to visible and infrared light, the use of UV-transmissive filters that also block a broad range of visible and infrared light is necessary to reduce ambient background and thereby enable alpha imaging. For environments without a UV background, like indoor LED lighting, the 337.1 nm emission can be effectively used to detect alpha sources. A novel 'sandwich' filter structure, incorporating an absorptive filter between two interference filters, has been developed to minimize multi-reflection between interference filters and enhance blocking efficacy. This setup enabled successful imaging of a 29 kBq alpha source from a distance of 3 meters within 10 minutes. It has also proven highly effective within the confines of a glovebox with an acrylic window, which filters most of the ambient UV background outside the glovebox [21].

For outdoor imaging, the UV background cannot be ignored. Even at night, the moonlight, city light or astronomical twilight all have spectral components at 337 nm. Daytime imaging presents additional challenges due to overwhelming UV constituents of sunlight. The UVC region (200 to 280 nm) is largely free from solar interference due to atmospheric absorption of shortwavelength, UV light by oxygen and ozone. This offers a 'solar-blind' window for outdoor alpha RL detection. However, RL emissions in this spectrum are weak, constituting less than 1% of total emissions, predominantly generated by trace amounts of nitric oxide (NO) in the air [17,22]. Unfortunately, the effective sandwich filter configuration is infeasible for UVC imaging as there are no commercially available absorptive filters with sufficient transmission in the UVC range and broadband blocking across the visible and infrared regimes.

Recent experiments have explored using PMTs to detect the UVC emissions of alpha RL [10, 11]. However, these experiments are still under controlled indoor lighting conditions, limiting their application in real world settings. Additionally, PMTs require a narrow field-of-view and a scanning mechanism to locate alpha sources over large areas, processes which can be labour-intensive and time-consuming.

2. Materials and Methods

2.1. Alpha Sources

For the experiments, an Americium-241 (Am-241) alpha source with an activity of 3 MBq and an active area of 12.5 mm diameter was employed. Am-241 typically emits alpha particles with an energy of 5.5 MeV. In this experimental setup, the alpha source was sealed beneath a thin gold film which slightly reduced the alpha energy to 4.7 MeV.

The alpha source includes a white polypropylene plastic sealing ring around the active area. The entire source was mounted on a stand fabricated from polylactide using a 3D printer. Adjacent to

 doi:10.20944/preprints202407.1264.v1

the alpha source, a metal bolt was placed to act as a control surface. The configuration of the setup is depicted in Figure 1.

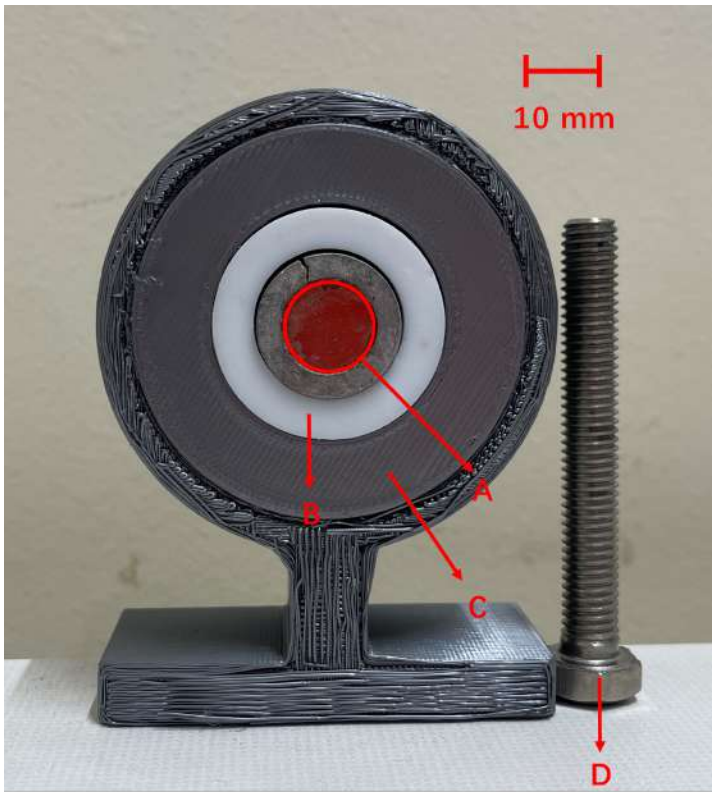

Figure 1. Detailed view of the alpha source setup: (A) active area, (B) plastic ring, (C) 3D printed polylactide stand, and (D) control surface bolt.

2.2. Detection System

Camera

The detector was a deep cooled iKon-M 934 BU2 (*Oxford Instruments Andor, Belfast, UK*) CCD. It originally has 1024 × 1024 pixels. In order to reduce the read noise per pixel, during the experiment, a 8 × 8 pixel binning was used. Therefore, the resultant resolution is 128 × 128 pixels. During the experiment, the camera is cooled to -90 degree. The quantum efficiency (QE), which is the measure of the effectiveness of an imaging device to convert incident photons into electrons, is around 60% in 200 nm - 400nm.

2.3. Filter Selection

A diverse array of optical filters was selected to optimize detection capabilities and control environmental interference during the experiment. The details of each filter are provided in the Table 1:

 doi:10.20944/preprints202407.1264.v1

Table 1. Summary of optical filters used in the experiment. CWL: Center Wavelength, FWHM: Full Width at Half Maximum, OD: Optical Density.

Filter Name	Supplier	Specifications	Purpose
65–128	Edmund Optics, York, UK	Reflective filter, CWL: 337 nm, FWHM: 10nm, OD: 4	Used to detect alpha RL at 337 nm.
39-343	Edmund Optics, York, UK	Reflective filter, CWL: 343 nm, FWHM: 5nm, OD: 4	Employed to detect background radiation at 343 nm.
Hoya U340	UQG Ltd., Cambridge, UK	Absorptive filter, bandpass: 275–375 nm	Served to reduce multi-reflection between reflective filters.
FF01-276/SP-25	Laser 2000 Photonics, Cambridge, UK	Reflective filter, 276 nm short pass	Utilised to eliminate ambient sunlight interference.
FBH450-40	Thorlabs Ltd., Lancaster, UK	Reflective filter, CWL: 450 nm, FWHM: 40 nm, OD: 5	Captures images in the visible band to overlap with the alpha RL signal.

Figure 2 illustrates the transmission characteristics of these filters across their respective wavelength ranges.

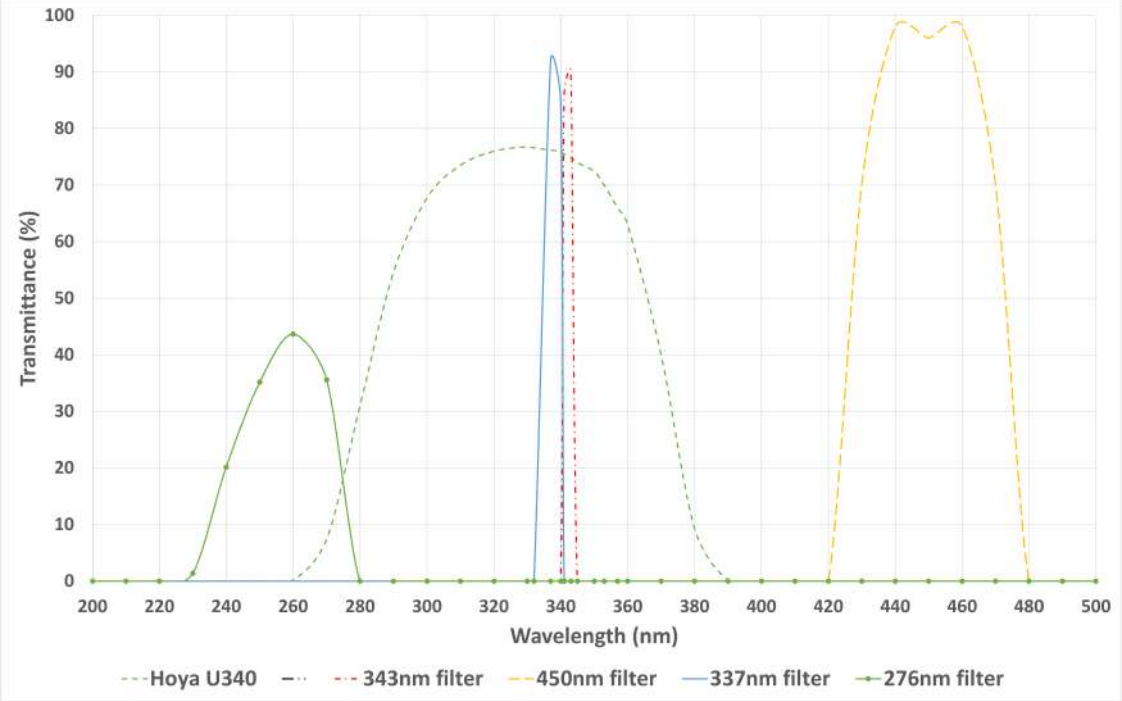

Figure 2. Graph showing the transmission versus wavelength for each filter used in the experiment.

2.3.1. Filter System for Nighttime Imaging

For nighttime imaging, where the ambient UV background is significantly reduced, the 337 nm center wavelength (CWL) filter was employed to capture the primary emission of alpha RL. Unlike the distinct peaks characteristic of alpha RL, the UV background at night, such as moonlight or reflections from city lights and sunlight, typically exhibits a continuous broad emission spectrum. To effectively manage any residual UV background, the 343 nm CWL filter was utilized for background subtraction. The filter's transmission characteristics are similar to those of the 337 nm filter, which means it captures similar UV background. However, it crucially excludes any alpha RL emission peaks, making it highly effective for subtracting background UV influences.

 doi:10.20944/preprints202407.1264.v1

The filters were arranged in a sandwich structure, as depicted in Figure 3, to enhance the blocking rate of the system. This configuration incorporated an absorptive filter between two reflective (or interference) filters to minimize multi-reflections and enhance image clarity [21].

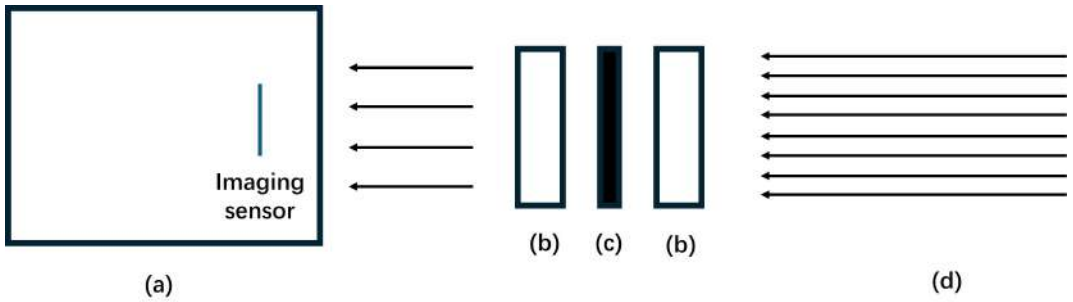

Figure 3. Illustration of the sandwich filter structure: (a) CCD and imaging sensor; (b) two reflective filters, either 337 nm CWL or 343 nm CWL used in this experiment; (c) an absorptive filter, specifically a Hoya U340 used here; (d) direction of incoming light.

2.3.2. Filter System for Daytime Imaging

During daytime, imaging under sunlight poses a challenge due to overwhelming UV background when using a 337 nm filter. Here, 276 nm short pass filters were utilized to reject sunlight effectively. However, a single 276 nm filter is insufficient to completely block sunlight. To overcome this, filters were stacked and each was tilted using a 3D-printed spacer with 10 degree angle. This setup reduces multi-reflections by redirecting stray light off-path and into the lens tube after a few reflections, thereby improving filter effectiveness. A sandwich structure was not used here because an absorptive filter with good UVC transmission and high blacking rate in visible and infrared region was not found. A total of five 276 nm filters were stacked to ensure thorough sunlight exclusion. A diagram demonstrating the theory behind the filter tilting and the specific arrangement used is shown in Figure 4.

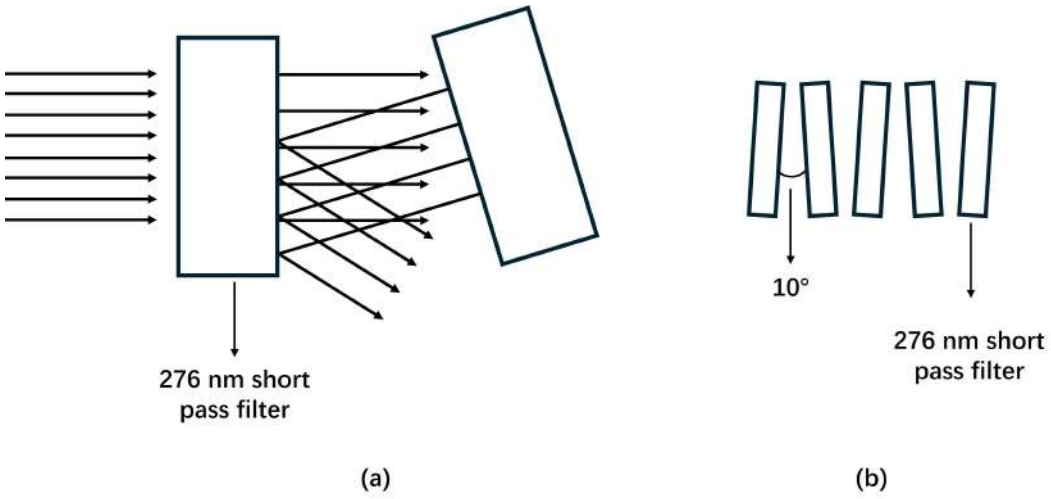

Figure 4. (a) By tilting the filters, light that might otherwise reflect between them is directed off-path. After a few reflections, this stray light is absorbed by the lens tube, thereby reducing the light-bunching effect; (b) Arrangement of the stacked five 276 nm short pass filters for sunlight detection.

2.3.3. Optical Configuration

For the optical setup of this experiment, a triplet lens system was designed. The specifications of each lens are summarized in Table 2.

Each lens was constructed from UV fused silica to maximize the transmission of the alpha RL signal. An anti-reflection coating was applied to each lens to further enhance transmission efficiency

 doi:10.20944/preprints202407.1264.v1

and image quality. To further improve image quality, an aspheric lens (21-912, Edmund Optics, York, UK) was selected as the imaging lens. The entire lens assembly was housed in standard lens tubes provided by Thorlabs Ltd., Lancaster, UK. The assembly configuration, including the position of lenses and filters, is detailed in Figure 5.

Table 2. Specifications of optical lenses used in the experiment. FL: Focal Length.

Lens Name	Supplier	Specifications
LA4372-UV	Thorlabs Ltd., Lancaster, UK	FL = 150.0 mm, Aperture = 75 mm
LC4513-UV	Thorlabs Ltd., Lancaster, UK	FL = -75.0 mm, Aperture = 25.4 mm
21-912	Edmund Optics, York, UK	FL = 25 mm, Aperture = 25 mm

A key design criterion was to ensure that incoming light rays in the space allocated for the filter arrangement (Figure 5(c)) were approximately normal to the filter surfaces. This orientation minimizes the risk of blue shift, which could otherwise impact the fidelity of the wavelength detection. The entire system is characterized by an f-number of approximately 0.5, and a field of view of 10 degrees.

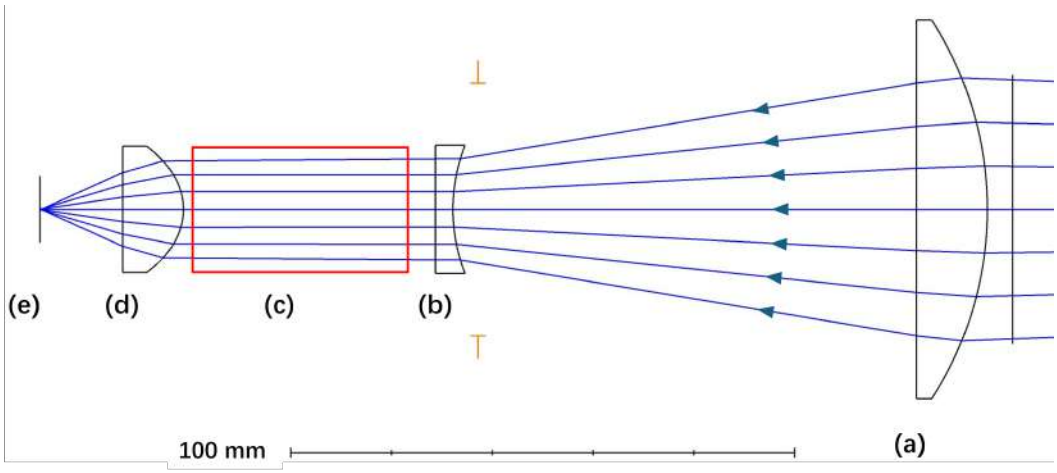

Figure 5. Configuration of the lens system: (a) LA4372-UV, (b) LC4513-UV, (c) space allocated for filter arrangement as depicted in Figures 3 and 4, (d) 21-912, and (e) the image sensor of the camera.

The overall assembly of the alpha camera is shown in Figure 6, the total weight is about 3 kg.

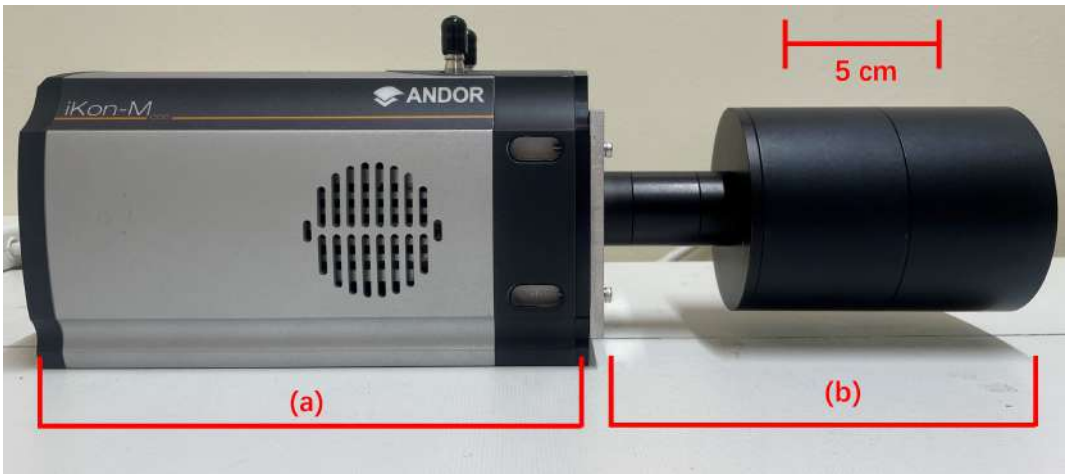

Figure 6. Comprehensive view of the alpha camera setup: (a) iKon 934 CCD camera (b) Integrated lens and filter system.

 doi:10.20944/preprints202407.1264.v1

2.3.4. Power Supply

Given the lack of readily available power sources in open outdoor environments, a Jackery Explorer 240 portable power station (Jackery, Oakland, CA, USA) was employed to provide power to the camera system. This power supply offers an operational duration of approximately four hours, ensuring continuous functioning during field experiments.

2.3.5. Artificial Light Source

To simulate the ambient light conditions typical of urban environments during nighttime imaging, several artificial light sources were utilized. The specifications of these light sources are summarized in Table 3:

Table 3. Specifications of artificial light sources used in the experiment.

Light Source	Supplier	Specifications
Fluorescent Light Tube	Megaman, Herts, UK	20 watts, 1151 lumen
Incandescent Light Bulb	Leuci, Buckinghamshire, UK	40 watts, 389 lumen
LED Light Bulb	Wilko, Bristol, UK	4.4 watts, 470 lumen

2.4. Image Acquisition and Processing

The lens arrangement remained consistent across both daytime and nighttime imaging sessions. The primary difference lay in the choice of filters: 337 nm and 343 nm for nighttime and 276 nm short pass for daytime. The detection distance, which is the distance between the front of the camera lens and the alpha source, was set at 1 meter for nighttime imaging and 70 cm for daytime imaging. This variance is attributable to the uncorrected chromatic aberration in the lens system which affects the focal distance, and therefore the sample distance need to be changed for detecting signal at different wavelengths.

Image exposures were several minutes. Raw images were converted from the proprietary format to CSV files using Andor SOLIS software (version 4.30.30024.0). Given the prolonged exposure times, cosmic rays and gamma rays from the Am-241 source introduced significant noise, appearing as intense peaks in individual pixels. To address this, a median filter with a 3×3 kernel (Python 3.11.9, scipy.ndimage package) was applied to all images.

Nighttime Imaging: For nighttime imaging, the sandwich filter configuration centered at 337 nm was utilised to capture the main alpha RL emission. Subsequently, the 343 nm centered sandwich filter was used to acquire the background image. The positions of both the camera and the source remained unchanged during filter exchanges. The background image was scaled so that its maximum intensity matched that of the signal image. This scaling was necessary to compensate for the difference in FWHM between the two filters, ensuring consistent background intensity across both images. The alpha RL signal was then isolated by subtracting the 343 nm background image from the 337 nm emission image. During this subtraction, any pixel values resulting in less than zero were set to zero, to avoid negative intensity values that are not physically meaningful.

Daytime Imaging: In daytime conditions, the alpha RL was directly captured using a stack of five tilted 276 nm short pass filters designed to reject sunlight effectively and capture the alpha RL in UVC range. No background subtraction was required for daytime imaging as the indirect sunlight captured did not significantly affect the alpha RL detection.

Post-processing involved representing the RL signal using a colormap, which was then superimposed on the grayscale visible light image (captured using the 450 nm FBH450-40 filter) to accurately depict the location of the alpha source. This visualization was executed using Python 3.11.9 and the matplotlib package.

 doi:10.20944/preprints202407.1264.v1

3. Results and Discussion

3.1. Imaging of Alpha source at Nighttime

The nighttime experiments were conducted at Fenswood Farm, Bristol, UK, approximately 4.6 miles from the city center to minimize city light interference. Various artificial light sources (LED, fluorescent, and incandescent lamps) summarised in Table 3 were used to simulated different urban lighting conditions. The experiments took place from 00:00 AM to 2:00 AM on June 12th, 2024. During this period, astronomical dusk is not achieved, resulting in UV ambient background from sky illumination (astronomical twilight). The experimental setup is illustrated in Figure 7. The detection distance was 1 metre and the exposure time was 1 minute. The results are presented in Figures 8–11.

Without artificial lighting, substantial ambient UV light was detected by the 337 nm filter system. For instance, the white plastic ring around the alpha source's active area is reflective to UV light and appeared to register high counts, as shown in Figure 8(a). By subtracting the 343 nm background image, these ambient light patterns were effectively removed, isolating the alpha source signal as depicted in Figure 8(c).

With LED lighting, no additional UV background was observed, demonstrating the effectiveness of the filter system, as illustrated in Figure 9. In contrast, additional UV background was detected with incandescent and fluorescent light sources, shown in Figures 10 and 11, respectively. The incandescent source was placed 8 meters from the alpha source. The corresponding background image subtraction, allowed for the detection of the alpha source. However, when the fluorescent light was placed placed 8 meters from the alpha the source it produced an excessive UV background. As seen in Figure 11, this continued to overshadow the RL signal from the alpha source, even after background subtraction.

Figure 7. Experimental setup for nighttime imaging of alpha RL: (a) alpha source, (b) alpha camera, (c) controlling laptop, (d) distance between light bulb and alpha source, (e) power bank and supply, (f) light lamp simulating ambient light source.

 doi:10.20944/preprints202407.1264.v1

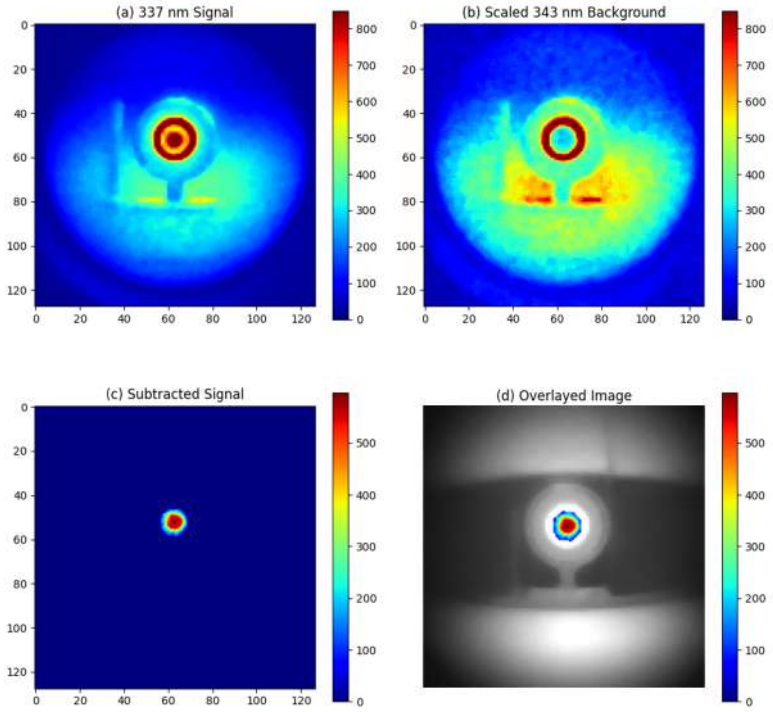

Figure 8. Experimental result for nighttime imaging of alpha source at 1 meter distance without artificial light source: (a) Signal image around 337 nm, (b) Background image around 343 nm, (c) Signal obtained by subtracting the 343 nm background from the 337 nm emission, (d) Overlay of the subtracted signal on a visible light image of the alpha source.

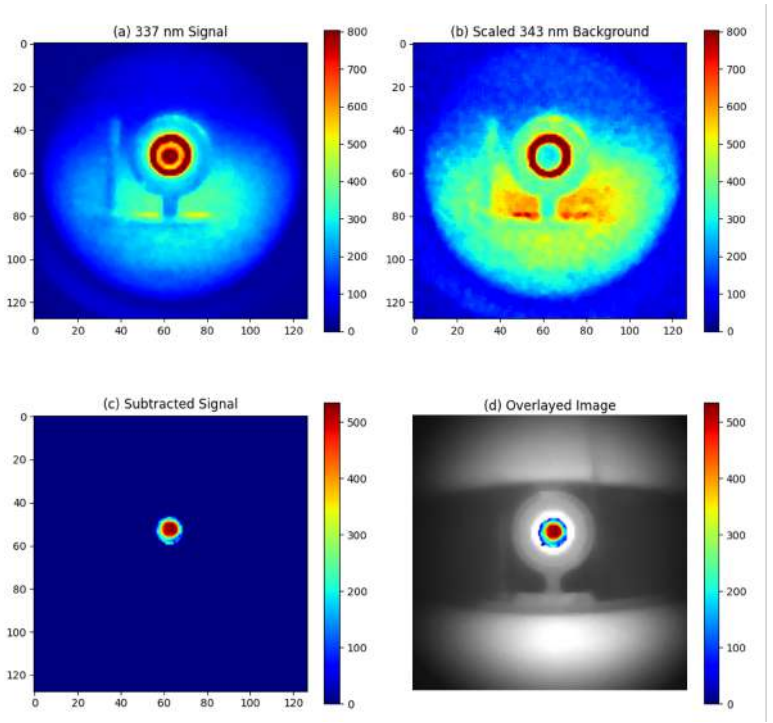

Figure 9. Experimental result for nighttime imaging of alpha source at 1 meter distance with an LED light source placed 1 meter away from the alpha source: (a) Signal image around 337 nm, (b) Background image around 343 nm, (c) Signal obtained by subtracting the 343 nm background from the 337 nm emission, (d) Overlay of the subtracted signal on a visible light image of the alpha source.

 doi:10.20944/preprints202407.1264.v1

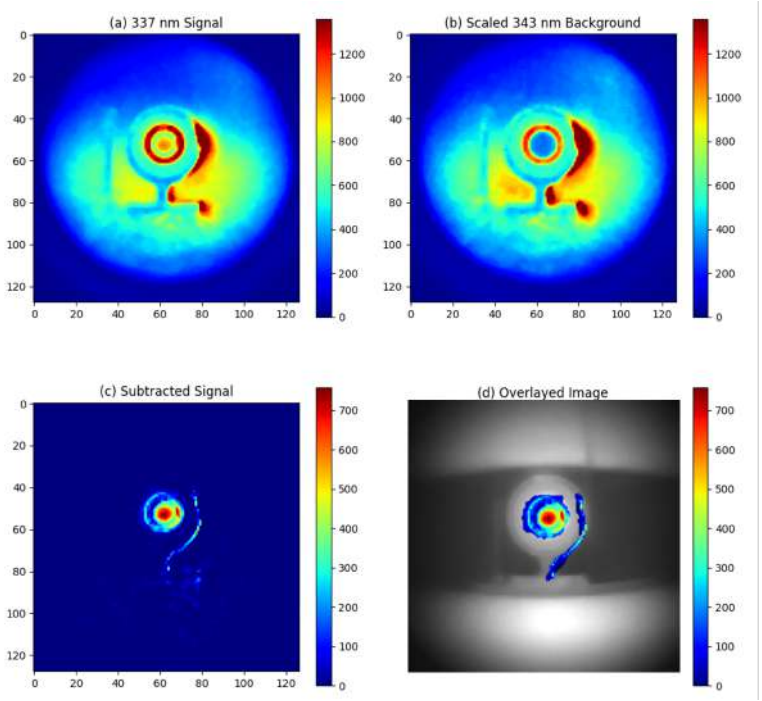

Figure 10. Experimental result for nighttime imaging of alpha source at 1 meter distance with an incandescent light source placed 8 meters away from the alpha source: (a) Signal image around 337 nm, (b) Background image around 343 nm, (c) Signal obtained by subtracting the 343 nm background from the 337 nm emission, (d) Overlay of the subtracted signal on a visible light image of the alpha source.

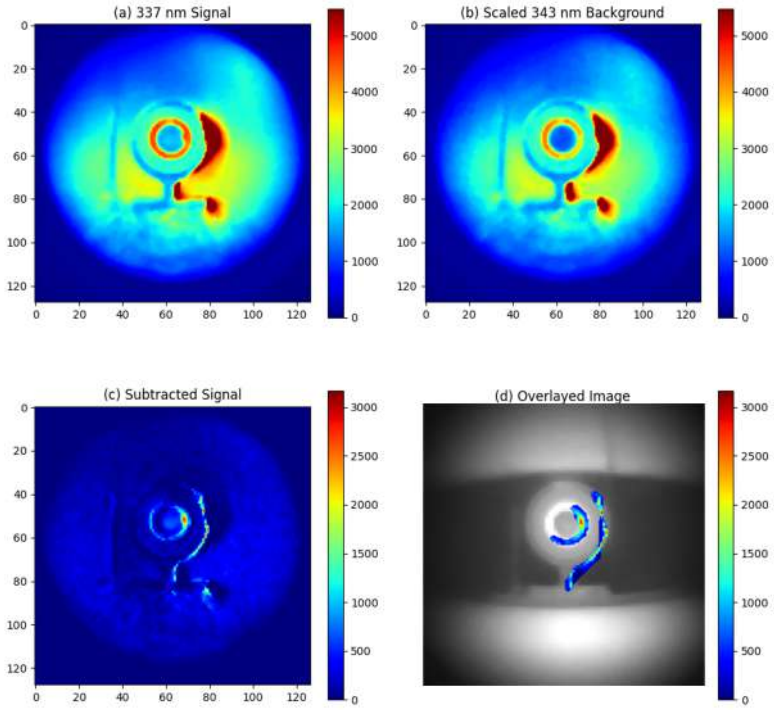

Figure 11. Experimental result for nighttime imaging of alpha source at 1 meter distance with a fluorescent light source placed 8 meters away from the alpha source: (a) Signal image around 337 nm, (b) Background image around 343 nm, (c) Signal obtained by subtracting the 343 nm background from the 337 nm emission, (d) Overlay of the subtracted signal on a visible light image of the alpha source.

 doi:10.20944/preprints202407.1264.v1

3.2. Imaging of Alpha Source at Daytime

Daytime experiments were conducted at Fenswood Farm, Bristol, UK, at 15:00 on June 12th, 2024, under cloudy conditions. The setup for these experiments is illustrated in Figure 12. The camera was positioned to avoid directly facing toward the sun, capturing only indirect sunlight reflected from the ground and walls. The detection distance was 70 cm and the exposure time was 10 minutes. This configuration allowed for clear visualization of the alpha source signal with signal to noise ratio (SNR) of about 3, as shown in Figure 13(a).

In contrast, when the camera faced direct sunlight, the intense ambient light overwhelmed the alpha source signal, making it indistinguishable, as shown in Figure 13(b). Despite the use of a stack of six 276 nm short pass filters, the direct sunlight background could not be adequately reduced. This suggests that a small amount of sunlight below 280 nm might be reaching the ground, bypassing the filter range. Further research is needed to verify this hypothesis.

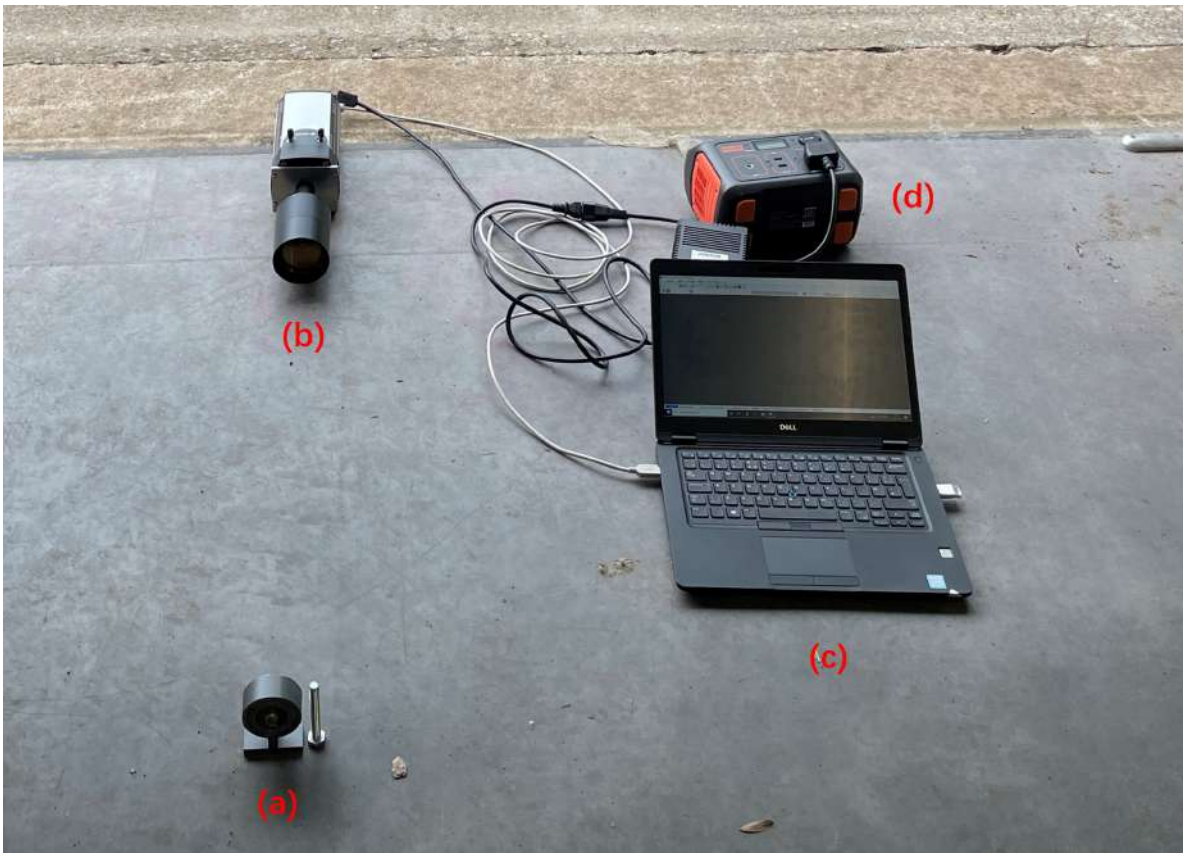

Figure 12. Experimental setup for daytime imaging of the alpha source: (a) Alpha source, (b) Alpha camera, (c) Controlling laptop, (d) Power bank and supply.

 doi:10.20944/preprints202407.1264.v1

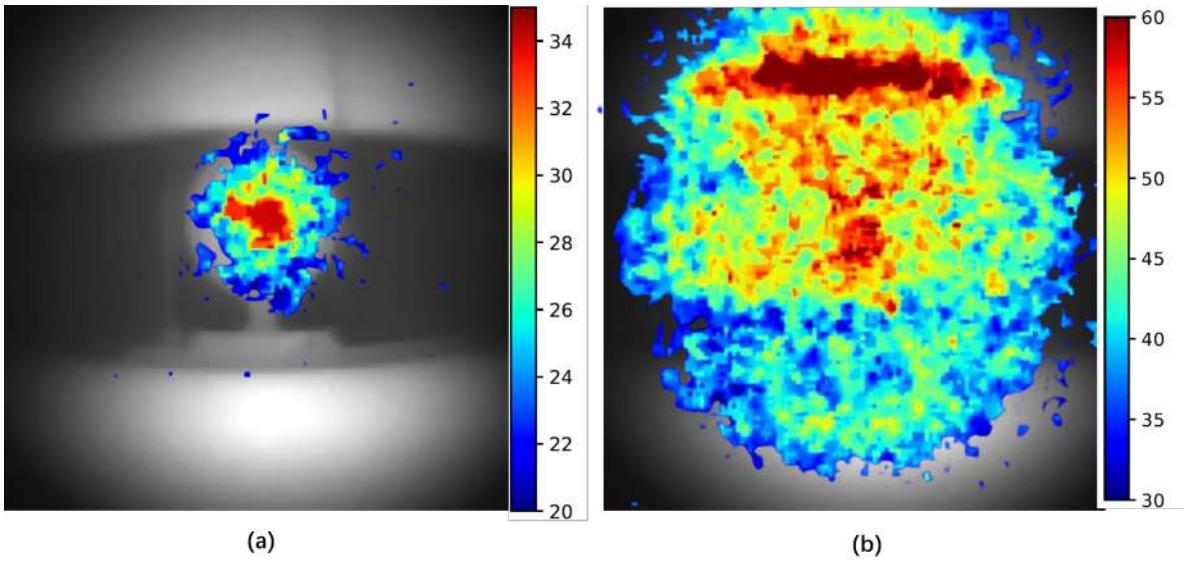

Figure 13. Experimental results for daytime imaging of the alpha source at a 70 cm distance in 10 minutes. The alpha source signal is represented using a color map and overlaid on a visible light image of the alpha source. (a) Under indirect sunlight, the alpha source signal is clearly visible. (b) Under direct sunlight, the ambient background overwhelms the signal, making it undetectable.

4. Conclusion

This study successfully demonstrated the capability of long-range imaging of a relatively weak alpha-emitting radiation source through radioluminescence (RL) in an open environment under varying lighting conditions. Conducted at Fenswood Farm, Bristol, UK, the experiments provided clear insights into the challenges and capabilities of detecting alpha RL signals both during nighttime and daytime conditions. This achievement is highly desirable for the nuclear industry, where such capabilities can significantly enhance safety and monitoring processes.

During nighttime imaging, a sandwich filter system was employed to enhance the blocking ability. The filter centered at 337 nm captured the main emission of alpha RL, while a filter system centered at 343 nm facilitated background subtraction. The effectiveness of this filter system was confirmed as it successfully isolated the RL signal of a 3 MBq alpha source from ambient UV light at a 1 meter detection distance within one minute. Different controlled artificial lighting sources were tested to simulate city light. Notably, the LED light source did not introduce additional UV background, pragmatically confirming that alpha imaging is viable within nuclear facilities when LED lighting is used. However, both incandescent and fluorescent lights posed challenges due to their inherent UV emissions, with the fluorescent lighting proving particularly problematic by overwhelming the alpha RL signal even after background subtraction.

During daytime experiments, a stack of five tilted 276 nm short pass filters was used to reject sunlight background and capture alpha RL in the UVC region. This camera setup could detect a 3 MBq alpha source at 70 cm in 10 minutes under indirect sunlight. Direct sunlight, however, masked the alpha RL signal, emphasizing the need for careful planning of outdoor RL imaging applications.

These findings highlight the potential of RL imaging systems for environmental monitoring and scientific research in conditions that closely mimic real-world scenarios. To our knowledge, the alpha camera described in this paper is the most capable alpha RL imaging system ever demonstrated. Future work will focus on improving the filter systems for enhancing ambient light rejection under direct sunlight and optimizing lens configurations to enhance detection capabilities. Additionally, exploring more sophisticated image processing techniques could further mitigate the impact of background noise.

The implications of this research extend into areas such as environmental monitoring, nuclear safety, and forensic science, where accurate and efficient detection of radioactive materials under

 doi:10.20944/preprints202407.1264.v1

diverse environmental conditions is critical. The continued development and refinement of this technology promises to broaden its applicability and effectiveness in these vital fields.

Author Contributions: Conceptualization, Lingteng Kong, Thomas Scott, John Day and David Megson-Smith; Data curation, Lingteng Kong; Formal analysis, Lingteng Kong; Funding acquisition, Lingteng Kong, Thomas Scott, John Day and David Megson-Smith; Investigation, Lingteng Kong, Thomas Scott, John Day and David Megson-Smith; Methodology, Lingteng Kong, John Day and David Megson-Smith; Project administration, Lingteng Kong, Thomas Scott, John Day and David Megson-Smith; Resources, Lingteng Kong, Thomas Scott, John Day and David Megson-Smith; Software, Lingteng Kong and David Megson-Smith; Supervision, Thomas Scott, John Day and David Megson-Smith; Validation, Lingteng Kong, John Day and David Megson-Smith; Visualization, Lingteng Kong; Writing – original draft, Lingteng Kong; Writing – review & editing, Thomas Scott, John Day and David Megson-Smith.

Funding: This research was funded by PhD Scholarship (No. 202008060208, China Scholarship Council, Beijing, China. University of Bristol, Bristol, UK), Game changers program (No. GC692, Sellafield Ltd., Warrington, UK), Nuclear Security Science Network (NuSec) (ST/S005684/1, Science and Technology Facilities Council (STFC), Swindon, UK)

Institutional Review Board Statement: Not applicable.

Informed Consent Statement: Not applicable.

Data Availability Statement: Data are contained within the article.

Conflicts of Interest: The authors declare no conflicts of interest. The authors declare that this study received funding from Game Changers project of Sellafield Ltd. The funder was not involved in the study design, collection, analysis, interpretation of data, the writing of this article or the decision to submit it for publication. Patent: Lingteng Kong, John Charles Clifford Day, David Andrew Megson-Smith: UK Patent Application GB2316225.8 IMAGING OF ALPHA EMITTERS The University of Bristol. Name of inventors: Lingteng Kong, David Andrew Megson-Smith, John Charles Clifford Day. Status of application: Pending. Specific aspects of manuscripts covered in the patent application: The design of the alpha camera, filter system and process algorithm.

Abbreviations

The following abbreviations are used in this manuscript:

RL	Radio-luminescence
PMT	Photomultiplier tube
CCD	Charge-coupled device
CWL	Center Wavelength
FWHM	Full Width at Half Maximum
OD	Optical Density
FL	Focal Length
UV	Ultraviolet

References

1. Knoll, G.F. *Radiation detection and measurement*; John Wiley & Sons, 2010.
2. Loucas, B.D.; Durante, M.; Bailey, S.M.; Cornforth, M.N. Chromosome damage in human cells by γ rays, α particles and heavy ions: track interactions in basic dose-response relationships. *Radiation research* **2013**, *179*, 9–20.
3. Sawant, S.; Randers-Pehrson, G.; Geard, C.; Brenner and, D.; Hall, E. The bystander effect in radiation oncogenesis: I. Transformation in C3H 10T1/2 cells in vitro can be initiated in the unirradiated neighbors of irradiated cells. *Radiation research* **2001**, *155*, 397–401.
4. Harrison, J.; Fell, T.; Leggett, R.; Lloyd, D.; Puncher, M.; Youngman, M. The polonium-210 poisoning of Mr Alexander Litvinenko. *Journal of radiological protection* **2017**, *37*, 266.
5. Ihantola, S.; Sand, J.; Peräjärvi, K.; Toivonen, J.; Toivonen, H. Principles of UV–gamma coincidence spectrometry. *Nuclear Instruments and Methods in Physics Research Section A: Accelerators, Spectrometers, Detectors and Associated Equipment* **2012**, *690*, 79–84.
6. Inrig, E.; Koslowsky, V.; Andrews, B.; Dick, M.; Forget, P.; Ing, H.; Hugron, R.; Wong, L. Development and testing of an air fluorescence imaging system for the detection of radiological contamination. AIP Conference Proceedings. American Institute of Physics, 2011, Vol. 1412, pp. 393–400.

 doi:10.20944/preprints202407.1264.v1

7. Klose, A.; Luchkov, M.; Dangendorf, V.; Krasniqi, F.; Lehnert, A.; Walther, C. On the way to remote sensing of alpha radiation: radioluminescence of pitchblende samples. *Journal of Radioanalytical and Nuclear Chemistry* **2022**, *331*, 5401–5410.
8. Kume, N.; Sumita, A.; Sakamoto, N.; Hoshi, T.; Okazaki, K.; Miyadera, H.; Miyahara, Y.; Nakai, Y. Alpha emitter detection systems using a UV light detector. *Applied Optics* **2022**, *61*, 1414–1419.
9. Li, N.; Zhang, N. Remote detection of alpha radiation source by optical method. *Optoelectronics Letters* **2023**, *19*, 405–409.
10. Luchkov, M.; Dangendorf, V.; Giesen, U.; Langner, F.; Olaru, C.; Zadehrafi, M.; Klose, A.; Kalmankoski, K.; Sand, J.; Ihantola, S.; others. Novel optical technologies for emergency preparedness and response: Mapping contaminations with alpha-emitting radionuclides. *Nuclear Instruments and Methods in Physics Research Section A: Accelerators, Spectrometers, Detectors and Associated Equipment* **2023**, *1047*, 167895.
11. Sand, J.; Nicholl, A.; Hrnecek, E.; Toivonen, H.; Toivonen, J.; Peräjärvi, K. Stand-off radioluminescence mapping of alpha emitters under bright lighting. *IEEE Transactions on Nuclear Science* **2016**, *63*, 1777–1783.
12. Crompton, A.J.; Gamage, K.A.; Bell, S.; Wilson, A.P.; Jenkins, A.; Trivedi, D. First Results of Using a UVTron Flame Sensor to Detect Alpha-Induced Air Fluorescence in the UVC Wavelength Range. *Sensors* **2017**, *17*, 2756.
13. Baschenko, S.M. Remote optical detection of alpha particle sources. *Journal of radiological protection* **2004**, *24*, 75.
14. Chichester, D.L.; Watson, S.M. Multispectral UV-visual imaging as a tool for locating and assessing ionizing radiation in air. *IEEE Transactions on Nuclear Science* **2011**, *58*, 2512–2518.
15. Feener, J.S.; Charlton, W.S. Preliminary results of nuclear fluorescence imaging of alpha and beta emitting sources. 2013 3rd International Conference on Advancements in Nuclear Instrumentation, Measurement Methods and their Applications (ANIMMA). IEEE, 2013, pp. 1–8.
16. Kerst, T.; Sand, J.; Ihantola, S.; Peräjärvi, K.; Nicholl, A.; Hrnecek, E.; Toivonen, H.; Toivonen, J. Standoff alpha radiation detection for hot cell imaging and crime scene investigation. *Optical Review* **2018**, *25*, 429–436.
17. Krasniqi, F.S.; Kerst, T.; Leino, M.; Eisheh, J.T.; Toivonen, H.; Röttger, A.; Toivonen, J. Standoff UV-C imaging of alpha particle emitters. *Nuclear Instruments and Methods in Physics Research Section A: Accelerators, Spectrometers, Detectors and Associated Equipment* **2021**, *987*, 164821.
18. Sand, J.; Ihantola, S.; Peräjärvi, K.; Nicholl, A.; Hrnecek, E.; Toivonen, H.; Toivonen, J. Imaging of alpha emitters in a field environment. *Nuclear Instruments and Methods in Physics Research Section A: Accelerators, Spectrometers, Detectors and Associated Equipment* **2015**, *782*, 13–19.
19. Crompton, A.J. *Stand-off detection of alpha-induced air-radioluminescence even under daylight conditions*; Lancaster University (United Kingdom), 2019.
20. Dandl, T.; Heindl, T.; Ulrich, A. Fluorescence of nitrogen and air. *Journal of Instrumentation* **2012**, *7*, P11005.
21. Kong, L.; Scott, T.B.; Day, J.C.C.; Megson-Smith, D.A. Advancements in Remote Alpha Radiation Detection: Alpha-Induced Radio-Luminescence Imaging with Enhanced Ambient Light Suppression. *Sensors* **2024**, *24*, 3781.
22. Crompton, A.J.; Gamage, K.A.; Jenkins, A.; Taylor, C.J. Alpha particle detection using alpha-induced air radioluminescence: A review and future prospects for preliminary radiological characterisation for nuclear facilities decommissioning. *Sensors* **2018**, *18*, 1015.